Ultrahigh Vacuum Cryostat System for Extended Low Temperature Space Environment Testing

Justin Dekany, Robert H. Johnson, Gregory Wilson, Amberly Evans and JR Dennison

Abstract— **The range of temperature measurements have been significantly extended for an existing space environment simulation test chamber used in the study of electron emission, sample charging and discharge, electrostatic discharge and arcing, electron transport, and luminescence of spacecraft materials. This was accomplished by incorporating a new two-stage, closed-cycle helium cryostat which has an extended sample temperature range from <40 K to >450 K, with long-term controlled stability of <0.5 K. The system was designed to maintain compatibility with an existing ultrahigh vacuum chamber (base pressure $<10^{-7}$ Pa) that can simulate diverse space environments. These existing capabilities include controllable vacuum and ambient neutral gases conditions ($<10^{-8}$ to 10^{-1} Pa), electron fluxes (5 eV to 30 keV monoenergetic, focused, pulsed sources over 10^{-4} to 10^{10} nA-cm^{-2}), ion fluxes (<0.1 to 5 keV monoenergetic sources for inert and reactive gases with pulsing capabilities), and photon irradiation (numerous continuous and pulsed monochromated and broad band IR/VIS/UV [0.5 to 7 eV] sources). The new sample mount accommodates 1 to 4 samples of 1 cm to 2.5 cm diameter in a low temperature carousel, which allows rapid sample exchange and controlled exposure of the individual samples. Custom hemispherical grid retarding field analyzer and Faraday cup detectors, custom high speed, high sensitivity electronics, and charge neutralization capabilities used with <50 pA, <5 μs, $<3\cdot10^3$ electrons/pulse pulsed-beam sources permit high-accuracy electron emission measurements of extreme insulators with minimal charging effects. *In situ* monitoring of surface voltage, arcing, and luminescence (250 nm to 5000 nm) have recently been added.**

Index Terms—**materials testing, electron emission, space environment, low temperature, ultrahigh vacuum, cryostat, instrumentation**

I. Introduction

To better understand the effects of the space environment on materials used in spacecraft construction it is important to test these materials under highly controlled laboratory conditions. When simulating the space environment three key conditions to consider are pressure, radiation, and temperature. A space environment simulation chamber operating at ultrahigh vacuum with electron, ion and photon flux capabilities [1] has been extended to a wider operational temperature range allowing simulation of a broader range of space environment temperatures.

Electron transport and emission properties are central in understanding, modeling and mitigating spacecraft charging concerns; they are particularly susceptible to temperature changes, often exhibiting Arrhenius behavior ~[$(1/k_BT)$ exp$(-E/k_BT)$]. For example one of the mechanisms for exciting electrons into the conduction band is through thermal excitation [2]. As the temperature decreases, thermally excited electrons are less prone to move through an insulating material, leading to greater likelihood for charge build up. In the case of a spacecraft which is exposed to varying amounts of electron flux densities and electron energies, this environment can cause isolated regions made primarily of insulating material to electrostatically discharge. Electrical—and in some cases mechanical—failure caused by Electrostatic Discharge (ESD) is the leading source of damage to spacecraft due to the space environment [3]. Understanding these effects by better simulating the space environment over a broader range of temperatures encountered in space is the driving force behind these chamber modifications.

Research was supported by funding from the NASA Goddard Space Flight Center. Justin Dekany, Robert Johnson, Greg Wilson, Amberly Evans and JR Dennison are with the Materials Physics Group in the Physics Department at Utah State University in Logan, UT 84322 USA (e-mail: jdekany.phyx@gmail.com, bj68127@yahoo.com, GregdWilson@gmail.com, amb.eva@aggiemail.usu.edu, JR.Dennison@usu.edu). Dekany, Wilson and Evans are graduate students in the USU Physics Department. Dennison is a professor in that department. Johnson is an undergraduate student in the Mechanical Engineering Department at USU.

II. Experimental Test Chamber Design

An existing space environment simulation chamber has been designed to allow for a wide range of electron flux and energy bombardment while maintaining ultrahigh vacuum and continuous control of sample temperature. The capabilities of the chamber are summarized first. The focus of this paper is the design of the low temperature stage and the associate sample mounting system. An example of the use of the new low temperature stage for electron-induced luminescence and arcing experiments demonstrates the versitility of the design.

A. Electron Emission Test Chamber

The electron emission test chamber uses standard mechanical and turbomolecular pumps (V; see legend in Fig. 1) for roughing and an ion pump (W) for continuous maintenance-free operation (base pressure of $<10^{-7}$ Pa). Absolute pressure is monitored with Convectron and ion gauges (X). Partial pressure is measured with a residual gas analyzer (Y).

Electron flux is produced with a High Energy Electron Diffraction (HEED) gun (Kimball, Model EGPS-21B)1(A), which provides a monoenergetic beam with a flux of

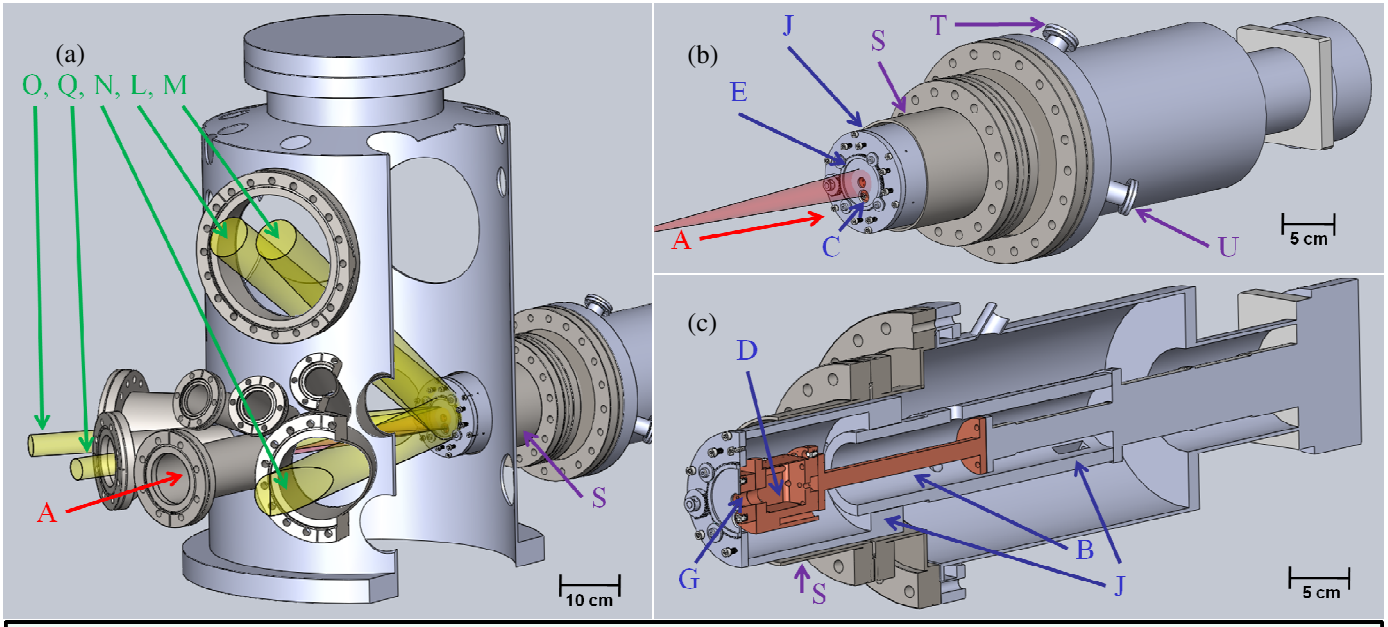

Radiation Sources
A Electron Gun

Sample Mount
B Sample Pedestal
C Sample
D Sample Mount
E Sample Mask Selection Gear
F Interchangeable Sample Holder
G *In situ* Faraday Cup
H Spring –Loaded Electrical Connections
I Temperature Sensor
J Radiation Shield

Analysis Components
K UV/Vis/NIR Reflectivity Spectrometers
L CCD Video Camera (400-900 nm)
M InGaAs Video Camera (800-1200 nm)
N InSb Video Camera (1000-5000 nm)
O SLR CCD Camera (300-800 nm)
P Fiber Optic Discrete Detectors
Q Collection Optics

Instrumentation (Not Shown)
Data Acquisition System
Temperature Controller
Electron Gun Controller
Electrometer
Oscilloscope

Chamber Components
R Multilayer Thermal Insulation
S Cryogen Vacuum Feedthrough
T Electrical Vacuum Feedthrough
U Sample Rotational Vacuum Feedthrough
V Turbomolecular/Mech. Vacuum Pump
W Ion Vacuum Pump
X Ion/Convectron Gauges – Pressure
Y Residual Gas Analyzer – Gas Species

Fig. 1. Experimental test chamber. (a) Chamber exterior view with cutaway showing the various analysis component lines of sight. The electron gun is positioned on axis with the sample plane. (b) Cryostat chamber mount, showing the electron beam trajectory (red). (c) Cutaway view of cryostat showing the first stage radiation shroud and second low temperature stage with sample mount and pedestal (red).

~1pA/cm^2 to 1 μA/cm^2 over an energy range of 5.00 to 30.00±0.01 keV. While the gun can produce a focused pulsed beam, for the experiments described here it was used in a continuous beam mode with a broad defocused beam of ~2 cm diameter FWHM. The current is monitored in real-time using an *in situ* Faraday cup (G) located in the center of the sample mount (D). Currents were measured using a fast, sensitive picoammeter with <0.2 pA resolution [5]. Additional lower energy electron gun sources (5 eV to 5 keV), ion sources (100 eV to 5 keV), and photon sources (~150 nm to 2000 nm) are also available in the chamber.

Light detection is accomplished with several cameras. All detectors have been calibrated *in situ* using NIST traceable methods, allowing for absolute spectral radiance values to be obtained. The cameras were positioned with views through vacuum port windows to get a clear view of the sample; this allowed for data collection of photon emission from the sample as a result of the cathodoluminessence and arcing caused by the electon beam interacting with the sample [4].

A Single Lens Reflex (SLR) CCD camera (O) (Cannon, EOS Rebel XT DS126071) took visible light data ranging from ~400 nm to 700 nm with 10 Mpixel images. The camera typically operates at 30 s shutter speeds at full aperture with a 55 mm lens, giving it an average spectral response of ~4·10^9 Counts/(W/cm^2·sr·μm). A CCD video camera (L) (Xybion, ISG-780-U-3) was sensitive to light from ~400 nm to 900 nm and collected data at 30 frames per sec. The spectral response for this detector is ~4·10^{10} Counts/(W/cm^2·sr·μm) using a 55 mm lens. An InGaAs video camera (M) was sensitive 800 nm to 1700 nm wavelengths, with maximum spectral response for longer wavelengths. This InGaAs video camera was operated at ambient room temperature collecting data at 60.1 frames per second. It has a spectral response of ~1·10^9 Counts/(W/cm^2·sr·μm) using a 35 mm lens. An InSb video camera (N) acted as a low spatial resolution IR detector (320x280 pixels). The photon response of this detector increases in sensitivity with increasing wavelength ranging from 1 μm to 5.5 μm. This camera operates at liquid nitrogen temperatures collecting data at varying integration times ranging from ~10 Hz to ~30 Hz depending on the band pass filters used. This detector has an spectral responsivity of ~7·10^7 Counts/(W/cm^2·sr·μm).

Two fiber optics-based spectrometers (K) provide Ultraviolet/Visible/Near Infrared photon spectral measurements from ~250 nm to 1700 nm. The UV/Vis spectrometer (Stellarnet, 13LK-C-SR; ~200 nm to 1080 nm) has a wavelength resolution of ~1 nm, while the NIR spectrometer (Stellarnet, RW-InGaAs-512; ~1000 nm to 1700 nm) has a ~3 nm resolution. Both detectors are housed in a piezoelectric cooler which maintains -20 K from ambient. A 4 cm diameter MgF collection optic gathers the light emitted by the sample and focuses the signal to a 1 μm fiber optic cable routed to the spectrometers.

Although not used for the measurements described in this paper, the new cryostat/sample mount is compatible with electron detection capabilities as well. The primary detector for emission studies is a custom hemispherical grid retarding field analyzer (HGRFA), with a retarding-field analyzer grid system for emitted-electron energy discrimination between

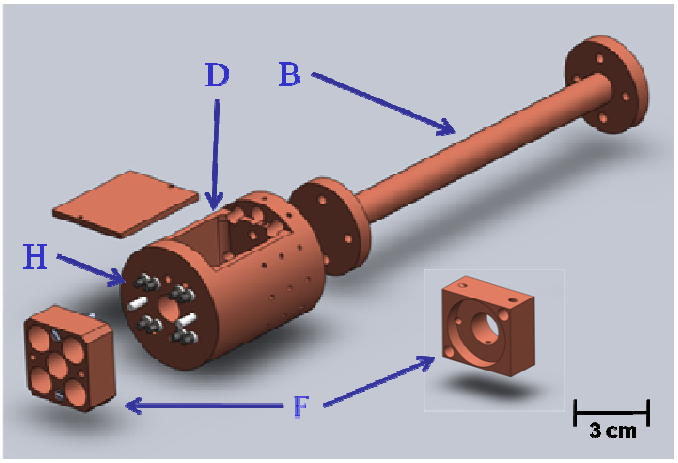

Fig. 3. View of cryostats second stage sample pedestal and interchangeable sample holder which attaches to the cryostat. Shown is a sample holder for four 1 cm diameter samples and a central Faraday cup and for a single 2.5 cm diameter sample.

backscattered electrons (energies >50 eV) and secondary electrons (energies <50 eV). By ramping the grid bias, energy spectra of the emitted electrons can also be measured using this detector. The HGRFA features a fully-encasing hemispherical collector for full capture of emitted electrons, that is particularly well suited and calibrated for absolute yield measurements. The HGRFA can be positioned in front of a single sample mounted at the end of the cryostat.

B. Low Temperature Stage Design

A closed-cycle helium cryostat has been added to the space environment simulation chamber to extend the operational temperatures for sample testing from <40 K to >450 K. Temperature is maintained to ±0.5 K using a standard computer-controlled PID temperature controller (RMC Cryosystems CR31-21) under Labview command and platinum RTDs (I) mounted on the sample holder, low temperature stage, and cryostat radiation shield. A large mass radiation shield (J) was attached to the cryostat's first stage (thermal load capacity of ~10 W at ~80 K) and a sample mounting stage was attached to the cryostats second stage (thermal load capacity of ~1 W at ~20 K); these large thermal masses helped maintain a constant sample temperature. Due to radiative heat transfer from the chamber walls, the addition of a multilayer thermal insulation blanket (R) wrapped around

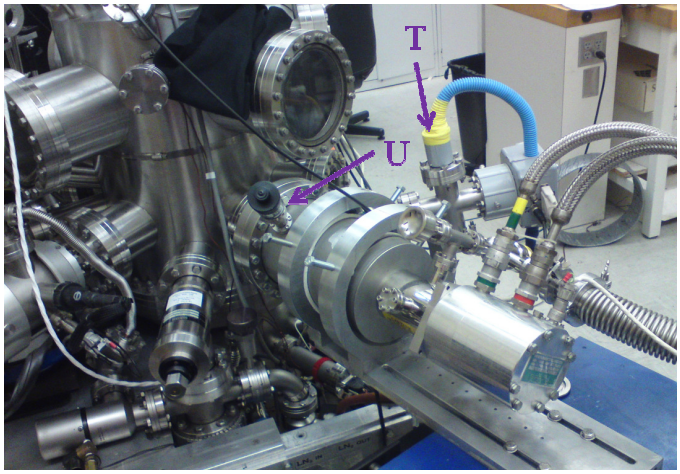

Fig. 2. Cryostat connected to the electron emission test chamber.

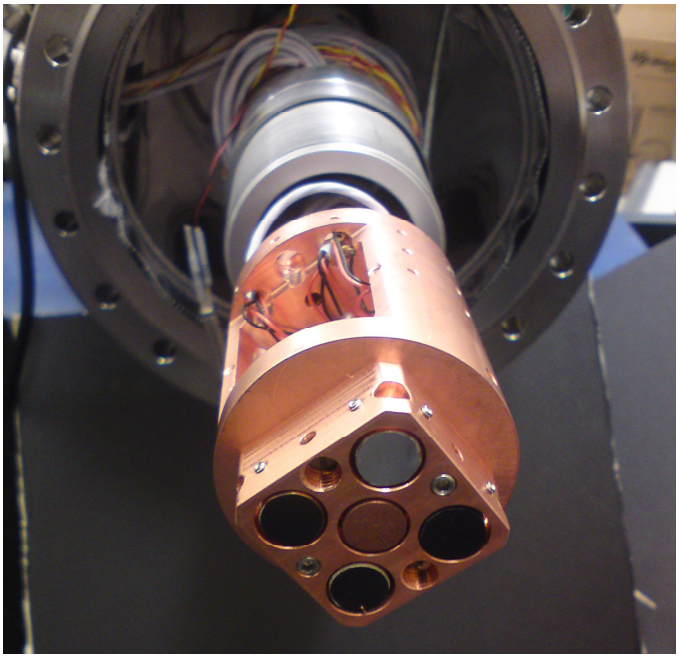

Fig. 4. Interchangeable sample holder with four 1 cm samples attached to the sample mount.

the first stage radiation shield (J) was required. This blanket consists of five sheets of thin conducting material separated by a thin mesh of insulating material. With this addition to the apparatus, the sample holder which is mounted to the cryostats second stage sample pedestal (B) can then reach 40 K, a temperature comparable to passively cooled spacecraft in standard orbit. Direct measurement of a sample confirmed a <2 K gradient between the samples and sample holder on which the temperature probe was mounted. Once the chamber was down to pressures of $<5\cdot10^{-3}$ Pa, the cryostat cooled the sample at a rate of ~ 1 K/min, reaching the lowest temperature of ~40 K in about 4 hr; this temperature can be sustained for weeks. Heating the sample is accomplished using a combination of control and bulk heaters attached to the radiation shroud and sample mount. Once activated, the temperature controller can heat the sample at a rate of ~ 1.5 K/min and can maintain any intermediate temperature from <40 to > 450 K. A typical cooling and heating profile is shown in Fig. 7.

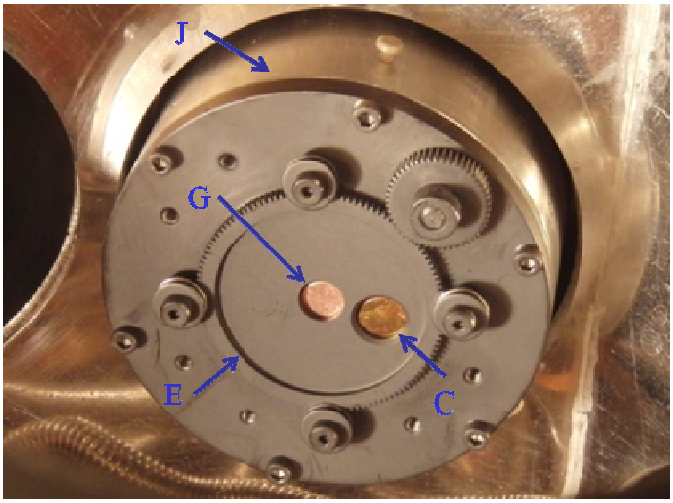

Fig. 5. Sample selection gear controlled using an external rotation translation (U). The gear/sample mask to access the Faraday cup (G) and one of four 1 cm diameter samples is shown.

The cryostat (see Fig. 1(b)) can be removed from the electron emission chamber and installed on other vacuum chambers that have an available 10 cm or 15 cm port.

C. Sample Carousel Design

The sample mount (D) has a versatile design that allows for a variety of configurations and sample sizes. Multiple sample holders (F) can be quickly interchanged with the use of spring-loaded, electrically-isolated electrode connectors (H), as shown in Fig. 3. The sample stage is electrically isolated with a Kapton spacer and PEEK screws, but maintains good thermal contact with the sample stage. The sample stage has a large wiring cavity (D) to facilitate various low-noise electrical connections, in addition to allowing room for bulk and control heaters.

In one configuration, four 1 cm diameter samples can be installed with an optional *in situ* Faraday cup (G) in the center location allowing for real-time monitoring of electron beam current (see Fig. 4). Samples in this configuration are mounted on (10.0 ± 0.1) mm diameter Cu cylinders, usually using UHV compatible, low-temperature, conductive epoxy (Masterbond, EP21TDCS-LO). The Cu cylinders are mounted in sample blocks using ceramic pins or 100 µm diameter sapphire spheres held in place with set screws to provide electrical isolation (see Fig. 4). Electrical connections to the sample are made via one or more spring loaded pins from the rear, allowing the sample current(s) to be monitored. Using this configuration, a sample mask selection gear (E) coupled to an external rotation translation feedthrough (U) allows masking of the samples not being tested (see Fig. 5); this minimizes potential sample charging of these samples. The sample masks also minimizes the amount of sample area exposed to the higher temperature chamber walls, since the mask is attached to the 80 K second stage of the cryostat. Larger samples of up to 2.5 cm in diameter or 2.5 cm by 2.5 cm square can be tested using a different sample mount (D), as shown in Fig. 6.

III. Applications

To highlight the capabilities of the low temperature cryostat incorporated into the space environment simulation test chamber, we present data from a study of the temperature dependence of electron-induced luminescence and arcing from spacecraft materials. With the various imaging detectors all focused at the sample (see Fig. 1(a)), a wide range of spectral analysis is possible [4]. Operation in a closed chamber in a dark room makes it possible to measure very low intensity sources.

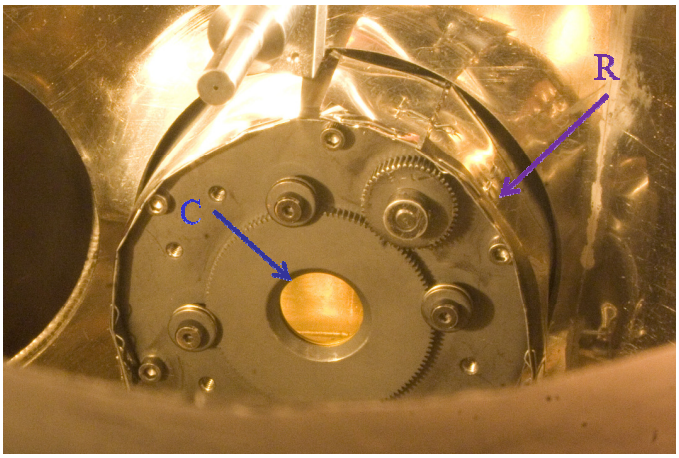

Fig. 6. Face plate with a 2.5 cm diameter sample mounted. Note radiation blanket wrapped around first stage radiation shield (J) of cryostat.

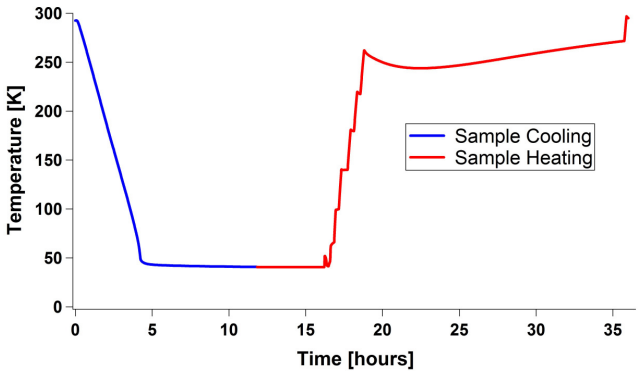

Fig. 7. Typical sample stage cooling and sample heating curves, with multiple sustained temperatures shown during heating cycle.

An example of this is shown in still frames captured with a CCD video camera. Figure 8(a) shows a 1 cm sample, which is illuminated using a dim fiber optic timing light to show the region to be exposed to the electron flux. Figures 8(b) and 8(c) show a comparison of the effect temperature has on this material; the glow at 293 K is hardly detected with this imaging camera, but as the temperature is decreased to 40 K intensity increases and a prominent glow is clearly evident. If enough charge is built up in the material arc events were observed [6] where the charge in the sample found a conduction path to the edge of the grounded sample holder (F). The very intense optical signature of the arc has been captured in a video frame shown in Fig. 8 (d). Figure 9 shows simultaneous measurements from an arc event as recorded by the electrometer and the CCD video camera. Here a constant current density of 1 nA/cm^2 was incident on the 1 cm sample and at ~91 s elapsed time the sample current spiked to over 40 nA. Additional measurements from a digital storage oscilloscope showed that these arcs were typically less than 1 µs in duration. The image from the CCD video camera

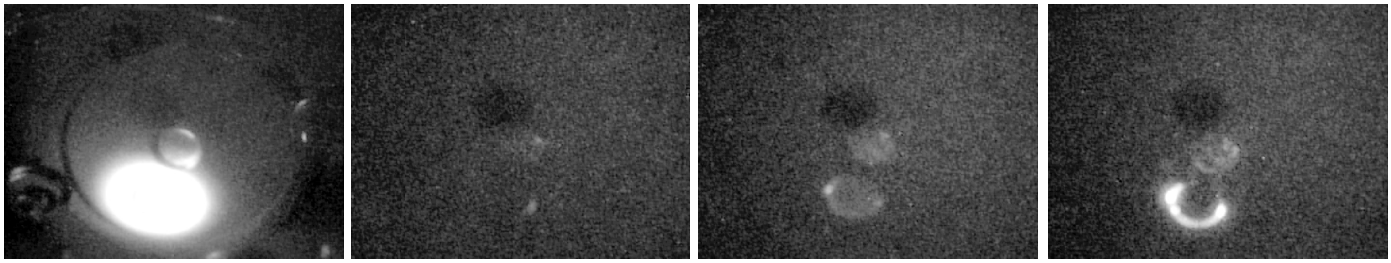

(a) (b) (c) (d)

Fig. 8. CCD video camera images (a) Timing light frame showing the sample location to be observed. (b) 293 K data with electron beam on sample. (c) 40 K data with electron beam on sample. (d) 40 K data with electron beam on sample showing an arc event.

provides optical confirmation of the electrical signature and provides additional information about the spatial location of the arc. Note the currents from the central region of the sample and from the sample edge region are measured independently, as shown in Fig. 9(b).

ACKNOWLEDGEMENT

We gratefully acknowledge contributions to instrumentation from Tamara Jeppsen of the Materials Physics Group, Michael Taylor for the use of infrared and CCD video cameras, and useful discussions with Robert Meloy and Charles Bowers of NASA Goddard Space Flight Center. This work was supported by a project for the James Webb Space Telescope Electrical Systems Group through the NASA Goddard Space Flight Center.

REFERENCES

[1] W.Y. Chang, J.R. Dennison, Jason Kite and R.E. Davies, "Effects of Evolving Surface Contamination on Spacecraft Charging," Paper AIAA-2000-0868, *Proceedings of the 38th American Institute of Aeronautics and Astronomics Meeting on Aerospace Sciences*, (Reno, NV, 2000).

[2] JR Dennison, "The Dynamic Interplay Between Spacecraft Charging, Space Environment Interactions and Evolving Materials," *Proc. of the* 12*th Spacecraft Charging Techn. Conf.,* (Kitakyushu, Japan, May 14-18, 2012).

[3] R.D Leach and M.B. Alexander, "Failures and anomalies attributed to spacecraft charging," NASA Reference Publication 1375, NASA Marshall Space Flight Center, August 1995.

[4] Amberly Evans, Gregory Wilson, Justin Dekany, Alec M. Sim and JR Dennison "Low Temperature Cathodoluminescence of Space Observatory Materials," *Proc. of the* 12*th Spacecraft Charging Techn. Conf.,* (Kitakyushu, Japan, May 14-18, 2012).

[5] C.D. Thomson, V. Zavyalov, and J.R. Dennison, "Instrumentation for Studies of Electron Emission and Charging from Insulators," *Proceedings of the 8th Spacecraft Charging Techn. Conf.* (NASA Marshall Space Flight Center, Huntsville, Al, October 2003).

[6] G. Wilson, JR Dennison, A. Evans and J. Dekany "Electron Energy Dependent Charging Effects of Multilayered Dielectric Materials" *Proc. of the* 12*th Spacecraft Charging Techn. Conf.,* (Kitakyushu, Japan, May 14-18, 2012).

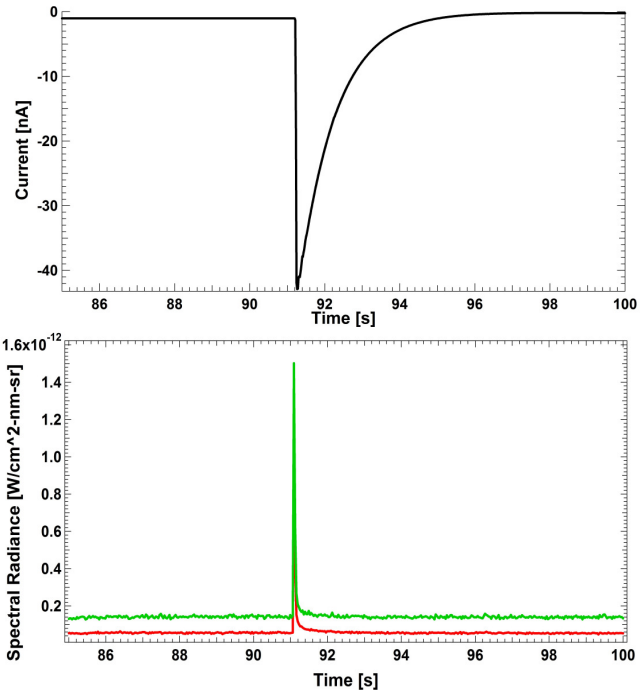

Fig. 9. Measured signatures of arcing. (a) Electrometer current data. (b) CCD Vis/NIR video camera integrated sample intensity data showing the increase in spectral radiance due to the arc event (surface glow data shown in **green**, edge glow data shown in **red**).

Justin Dekany is currently a graduate student at Utah State University in Logan, UT pursing an MS in physics. He received a BS degree in physics from USU in 2010. He has worked with the Materials Physics Group for four years on electron transport measurements, electrostatic discharge tests, electron emission measurements, and luminescence studies related to spacecraft charging. He has been the Lab Manager for the Materials Physics Group for the last two years.

Robert Johnson is currently a student in Mechanical Engineering at Utah State University, Logan. He has worked with the Materials Physics Group for a year on thermal vacuum chamber design related to spacecraft charging.

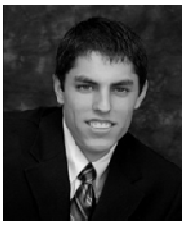

Greg Wilson is currently a graduate student at Utah State University in Logan, UT pursing an MS in physics. He received BS degrees in physics and mathematics from USU in 2011. He has worked with the Materials Physics Group for two years on electron emission and luminescence studies related to spacecraft charging. He also developed a composite model for electron range over a wide range of incident energies applicable to diverse materials.

Amberly Evans is currently a graduate student at Utah State University in Logan, UT pursing an MS in physics. She received BS degrees in physics and chemistry from USU in 2012. She has worked with the Materials Physics Group for five years on electron emission, luminescence and resistivity studies and on MISSE retrieval and post-flight analysis of *SUSpECS*. Much of her work has focused on optical scattering of spacecraft materials.

J. R. Dennison received the B.S. degree in physics from Appalachian State University, Boone, NC, in 1980, and the M.S. and Ph.D. degrees in physics from Virginia Polytechnic Institute and State University (Virginia Tech), Blacksburg, in 1983 and 1985, respectively. He was a Research Associate with the University of Missouri—Columbia before moving to Utah State University (USU), Logan, in 1988. He is currently a Professor of physics at USU, where he leads the Materials Physics Group. He has worked in the area of electron scattering for his entire career and has focused on the electron emission and resistivity of materials related to spacecraft charging for the last two decades.